Canadian Science Publishing

ARTICLE

# Dendroclimatic analysis of central Appalachian red spruce in West Virginia

Eric Yetter, Sophan Chhin, and John P. Brown

**Abstract:** We conducted dendroclimatic analyses and constructed future growth projections for red spruce (*Picea rubens* Sarg.) throughout the central Appalachians in the state of West Virginia. This study involved field sampling of 18 sites across red spruce's range in six regions throughout the Monongahela National Forest that were selected based on pairwise combinations of three latitudinal groups (north, central, and south) with two aspects (north and south). Each combination of latitudinal group and aspect was referred to as a landscape cluster. Growth was negatively impacted by high summer temperature stress but responded favorably to high fall temperatures. The results also suggested that red spruce was likely impacted by the degree of winter harshness in all landscape clusters. In the northern latitudinal landscape clusters, red spruce responded favorably to warm spring temperatures by allowing an early start to the growing season. Growth projections under a future climate change scenario show that future expected increases in mean and maximum monthly temperatures will have negative effects on future spruce growth. The forecasting results suggested that red spruce in northern latitudes on south aspects or central latitudes on north aspects are the landscape clusters that will likely be the most resilient to future climate change. Dendroclimatic results and future growth projections can assist with identifying locations that are most suitable for future red spruce restoration activities.

*Key words:* climate change, dendrochronology, red spruce, restoration.

**Résumé :** Nous avons effectué des analyses dendroclimatiques et avons établi des projections de la croissance future de l'épinette rouge (*Picea rubens* Sarg.) pour le centre des Appalaches dans l'État de la Virginie-Occidentale. Cette étude impliquait un échantillonnage sur le terrain de 18 stations à travers l'aire de répartition de l'épinette rouge dans six zones de la forêt nationale de Monongahela qui ont été choisies en fonction de combinaisons appariées de trois groupes latitudinaux (latitudes nord, centrale et sud) et de deux expositions (nord et sud). Nous faisons référence à un élément de paysage pour désigner chaque combinaison de groupe latitudinal et d'exposition. La croissance a été influencée négativement par les températures estivales élevées, mais a réagi positivement aux températures automnales élevées. Les résultats indiquent aussi que le degré de rigueur hivernale a probablement eu un impact négatif sur l'épinette rouge dans tous les éléments de paysage. Dans les éléments de paysage de latitude nord, l'épinette rouge a réagi positivement aux températures printanières élevées en démarrant hâtivement sa saison de croissance. Les projections de croissance selon un scénario de futurs changements climatiques montrent que les augmentations prévues de températures mensuelles moyenne et maximale auront des effets négatifs sur la croissance de l'épinette. Les résultats des prévisions indiquent que l'épinette rouge dans les latitudes nord exposées au sud de même que dans les latitudes centrales exposées au nord sont les éléments de paysage qui seront probablement les plus résilients aux futurs changements climatiques. Les résultats dendroclimatiques et les projections de croissance future peuvent aider à identifier les emplacements les plus appropriés pour les futures activités de restauration de l'épinette rouge. [Traduit par la Rédaction]

*Mots-clés :* changements climatiques, dendrochronologie, épinette rouge, restauration.



## 1. Introduction

Red spruce (*Picea rubens* Sarg.) was once very common in the central Appalachian Mountains but is now found in only a small portion (estimated to be as low as 7%) of its distributional range compared with the past (Rentch et al. 2016). Forest disturbance resulting primarily from anthropogenic causes such as fire and logging have been large contributors to the decline of red spruce (Blum 1990). Logging and wildfires collectively disturbed an estimated 97% of central Appalachian red spruce's distributional range throughout the 1800s and 1900s, with an estimate of over 580 000 ha of forest disturbed over the historical exploitation period (Thomas-Van Gundy and Sturtevant 2014). While fire and logging have contributed to the recent decline of red spruce, this was in addition to a long-term trend of population decline since the last ice age in the Appalachian region. The natural history of the region indicated that during the maximum extent of the last Wisconsin glaciation, red spruce was dominant in the central Appalachian region and occurred as open red spruce woodlands present at low elevations (Stephenson 2013). With the retreat of the ice sheet approximately 10 000 years ago, red spruce migrated north to more climatically suitable habitat. Relict populations of red spruce were left to persist at high elevations in the Appalachian region.

Received 18 November 2020. Accepted 5 April 2021.

**E. Yetter and S. Chhin.** Division of Forestry and Natural Resources, West Virginia University, 322 Percival Hall, 1145 Evansdale Drive, Morgantown, WV 26506, USA.

**J.P. Brown.** USDA Forest Service, Northern Research Station, 301 Hardwood Lane, Suite B, Princeton, WV 24740, USA.

**Corresponding author:** Sophan Chhin (emails: sophan.chhin@mail.wvu.edu; steve.chhin@mail.wvu.edu).





Published at www.cdnsciencepub.com/cjfr on 19 April 2021.

The restoration of red spruce in the central Appalachians is important because red spruce forests provide many ecosystem services. The endangered cheat mountain salamander (*Plethodon nettingi*) is endemic to red spruce associated forests in the state of West Virginia and within the central Appalachians (Pauley 2008). Increases in spruce cover may benefit cheat mountain salamander populations and may promote the expansion of the threatened Virginia northern flying squirrel (*Glaucomys sabrinus*), which relies on red spruce associated forests for food sources (Trapp et al. 2017). In addition, this habitat is critical for certain species of breeding birds and the sequestration of larger amounts of soil carbon compared with soils associated with hardwood forests (Nauman et al. 2015).

Dendrochronology is the science of dating tree rings to examine historical growth characteristics of trees (Speer 2012). Dendroclimatology is a more specific subdiscipline of dendrochronology that seeks to determine what climate factors have impacted tree growth (Fritz 1976). Results from dendroclimatic studies can be used to plan restoration activities and identify the suitability of future species in terms of climate change resilience (Chhin 2015). A dendroclimatic study that analyzes red spruce growth across the central Appalachians may highlight areas where red spruce growth will yield favorable growth rates given projections of future climate attributes. Studies in the central Appalachians have been mainly focused on other growth factors such as acid deposition, disturbance, and air pollution, but not specifically climate (Rentch et al. 2007; Mathias and Thomas 2018). Air pollution and associated acid rain historically contributed to growth declines in red spruce, but recent trends in air pollution reduction have resulted in growth increases (Kosiba et al. 2018). Mathias and Thomas (2018) found that central Appalachian red spruce has shown positive growth responses in the past 30 years due to decreases in air pollution and acid precipitation events. Mathias and Thomas (2018) also found that increases in mean July temperatures and increased $CO_2$ levels have had a fertilizer effect on red spruce growth.

Red spruce growth at the northern portion of its range (44.5–50°N) has shown growth increases with warmer temperatures and increased $CO_2$, but extremely warm temperatures may result in growth declines (Dumais and Prévost 2007; Kosiba et al. 2017). Red spruce near its southernmost range (35.6–39.1°N) in the southern Appalachians has different growth responses to climate variables than spruce at the northern portion of its range (Berry and Smith 2014; Koo et al. 2014; White et al. 2014; Walter et al. 2017). This difference in growth response may hint that the species could respond differently to climate in the isolated central Appalachian portion of its range. Increasing mean summer temperatures are having negative impacts on growth within red spruce's range in the southern Appalachians; future increases in temperature will likely reduce suitable habitat to higher elevations (Koo et al. 2014). Moisture stress is an additional factor that could contribute to spruce decline in the future (Berry and Smith 2014). Southern Appalachian red spruce relies on cloud cover for supplementary moisture from condensation that is necessary for growth (Johnson and Smith 2006). Cloud cover is important for sustaining spruce growth during the summer growing season as clouds mitigate negative growth effects associated with extreme summer temperature by limiting direct solar radiation and moisture loss (Berry and Smith 2014). Climate change predictions have estimated a reduction in cloudy days during the growing season in the southern Appalachians, and this reduction in cloud cover will also result in a reduction in moisture and habitat suitability in the south, particularly at lower elevations (Berry and Smith 2012). Although moisture deficits can be growth limiting to southern red spruce populations, excess moisture leading to anaerobic soil conditions in the spring also can have negative effects on growth; this could become even more of a factor considering future climate predictions (White et al. 2014). Overall, predictions of red spruce's growth response to increasing temperatures and moisture limitations forecast the reduction in suitable southern Appalachian red spruce habitat in the future (Walter et al. 2017).

Previous studies have established that the historical reach of red spruce extended to lower elevations than does its current range (Thomas-Van Gundy et al. 2012). Unfortunately, restoration efforts in low elevational areas could yield unfavorable results with future climate change (Rentch et al. 2007; Walter et al. 2017). For instance, future increases in mean summer temperatures from climate change may result in declines of spruce growth that are more noticeable at lower elevations (Gavin et al. 2008). In contrast, models created to help locate suitable lands for future red spruce restoration activities predict that restoration activities at higher elevations generally have higher likelihood of success (Thomas-Van Gundy and Sturtevant 2014). Red spruce at high elevations have benefited overall from warming, which may make the species better suited than its competitors at high elevations in the future (Kosiba et al. 2017).

Understanding how climate impacts growth would be helpful for future planning and resource allocation. In addition, determining how climate change may affect red spruce growth in the future could help guide restoration efforts in areas of the central Appalachians with the highest probability of spruce survival (Rentch et al. 2007; Walter et al. 2017). Consequently, the first objective of this study is to conduct dendroclimatic analysis to determine climate–growth relationships for central Appalachian red spruce. The second objective of this study is to project red spruce growth under a future climate change scenario. Projected growth rates will be compared with historic growth and used to estimate how central Appalachian red spruce growth may be affected by climate change.

## 2. Methods

### 2.1. Field sampling design

Most of the red spruce remaining in the central Appalachian Mountains occurs in West Virginia predominately on lands within the Monongahela National Forest (MNF). To take advantage of the large latitudinal range of red spruce forests in the MNF, this study included red spruce trees located throughout the extent of the national forest. Eighteen sites were randomly selected using Geographic Information System (GIS) software (i.e., ArcGIS) and the random sample tool located within the data management Arc toolbox (Theobald et al. 2007). The study area that was eligible for plot selection was determined by a forest type cover map obtained from the state of West Virginia's GIS clearinghouse website (Byers et al. 2013). All forested land with a minimum of 10% estimated red spruce cover according to the red spruce forest cover layer, was included for random plot placement (Fig. 1).

Six landscape clusters were established for 18 site locations (three sites per regional group). Landscape clusters organized individual sites based on their latitude and aspect. The landscape clusters are as follows: North Latitude and North Aspect (NLNA), North Latitude and South Aspect (NLSA), Central Latitude and North Aspect (CLNA), Central Latitude and South Aspect (CLSA), South Latitude and North Aspect (SLNA), and South Latitude and South Aspect (SLSA). Plot attributes for each landscape cluster are provided in Table 1. Regional grouping of sites by latitude ensures that plots within close spatial proximity are grouped together. Separating landscape clusters further by aspect (north aspect consists of azimuth of 0–45° and 315–360° while south aspect corresponds with 135–225° azimuth) ensures that variability in climate response is preserved as trees on north- and south-facing slopes may react differently to climate variables. Table 2 shows a breakdown of the individual sites within each region along with corresponding mean values.

At each site, 10 codominant and dominant red spruce trees were sampled within the 10-m-radius circular plot (0.0337 ha). A random bearing was established for each plot. Sampling started at the random bearing and then proceeded clockwise until the

**Fig. 1.** Maps showing (*a*) regional context of the study area in the midwestern and northeastern United States, and (*b*) a zoomed in view of the study area where dendroclimatic plots (black dots) were sampled in the Monongahela National Forest in West Virginia. These maps were created using ArcGIS® (version 10.8) software by Esri. ArcGIS® and ArcMap™ are the intellectual property of Esri and are used herein under license.

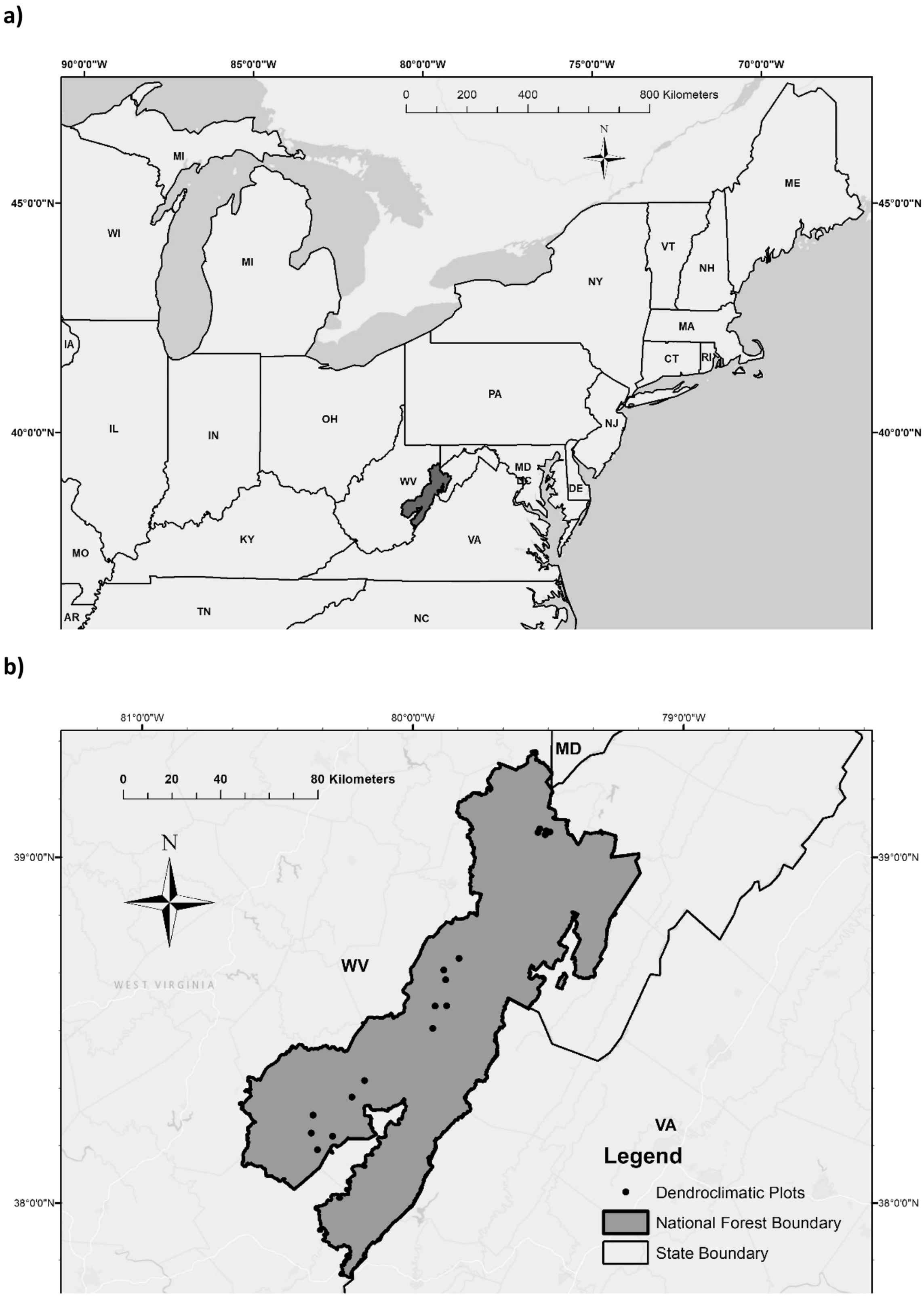

**Table 1.** Landscape clusters including the individual plots within each landscape cluster and their associated mean values for all three plots combined.

| Landscape cluster | Abbreviation | Plots | Latitude (°) | Longitude (°) | Elevation (m a.s.l.) | Temp. (°C) | Prec. (mm) | CMI | Soil drainage class | Diameter (cm) Avg | Diameter (cm) SE | Height (m) Avg | Height (m) SE | Plot basal area ($m^2 \cdot ha^{-1}$) Avg | Plot basal area ($m^2 \cdot ha^{-1}$) SE |
|---|---|---|---|---|---|---|---|---|---|---|---|---|---|---|---|
| North Latitude, North Aspect | NLNA | 8, 16, 147 | 39.0708, 39.0751, 39.0817 | −79.5383, −79.5078, −79.5311 | 1087 | 7.74 | 115.98 | 6.33 | Poor, Excessive, Poor | 44.01 | 1.35 | 23.30 | 0.34 | 31.91 | 1.32 |
| North Latitude, South Aspect | NLSA | 101, 115, 130 | 39.0645, 39.0727, 39.0720 | −79.5110, −79.4945, −79.4976 | 1091 | 7.74 | 115.98 | 6.33 | Well, Poor, Poor | 41.91 | 1.02 | 23.12 | 0.59 | 21.20 | 2.95 |
| Central Latitude, North Aspect | CLNA | 30, 85, 128 | 38.5710, 38.5715, 38.5063 | −79.9186, −79.8752, −79.9267 | 1272 | 7.14 | 125.98 | 8.06 | Mod. Well, Poor, Well | 44.59 | 1.36 | 23.80 | 0.65 | 26.02 | 1.55 |
| Central Latitude, South Aspect | CLSA | 13, 61, 103 | 38.6748, 38.6472, 38.7081 | −79.8864, −79.8793, −79.8302 | 1115 | 6.93 | 122.24 | 7.34 | Well, Mod. Well, Mod. Well | 47.58 | 2.09 | 23.09 | 0.50 | 25.56 | 2.03 |
| South Latitude, North Aspect | SLNA | 23, 113, 121 | 38.3552, 38.2031, 38.3076 | −80.1783, −80.3751, −80.2251 | 1206 | 7.82 | 113.18 | 8.05 | Well, Mod. Well, Well | 40.96 | 5.10 | 24.20 | 0.26 | 29.47 | 4.18 |
| South Latitude, South Aspect | SLSA | 40, 106, 142 | 38.2548, 38.1937, 38.1540 | −80.3686, −80.2963, −80.3525 | 1204 | 8.24 | 131.59 | 7.50 | Well, Mod. Well, Well | 43.80 | 1.81 | 24.10 | 0.15 | 32.53 | 1.10 |

**Note:** Temp., average annual temperature; Prec., annual average precipitation; CMI, average annual climate moisture index; all climate variables are reported for the 1981 to 2000 reference period. Soil drainage shows the expected soil drainage class from data obtained from USGS Soil Survey (websoilsurvey.nrcs.usda.gov): Mod. Well indicates soils in a moderately well drainage class; the soil drainage classes range from excessively well drained to very poorly drained. Avg is the average value of the three individual plot values. SE is the associated standard error values for the averaged data.

first 10 red spruce trees in the dominant or codominant size class were sampled. If the entire plot did not have 10 red spruce trees in the codominant or dominant size class, an additional 10 m was added to the plot radius and sampling continued, starting with the previous random bearing and proceeding clockwise. If necessary, additional 10 m segments were added to the plot radius until a total of 10 trees were sampled. The small sample size limitation of 10 trees was partly due to low density of red spruce observed at many of the red spruce sites. In addition, conservation concern for protecting red spruce habitat for the federally endangered cheat mountain salamander also limited sample size.

At each of the 18 plots, two increment cores were sampled at breast height (1.3 m) from each red spruce tree. The two cores were taken from the side of the stem perpendicular to the slope of the ground with the cores taken 180° from each other. Trees were sampled from the codominant and dominant height classes as we were concerned that intermediate and suppressed size classes may show less of a response to climate due to competition and growth suppression. Trees with noticeable defects or disease were not sampled. Additional data including diameter at breast height (DBH), total height, crown height, and bark depth, were collected for each sampled tree. Tree height and crown height were obtained using a hypsometer.

Since plot sizes were not uniform due to the variability of spruce density across the central Appalachians, stand densities were quantified for each sampled tree rather than at plot center. Basal area was determined around each cored tree. Basal area estimations were conducted using a 2.296 metric basal area factor (BAF) wedge prism. Ideal basal area calculation would be conducted using the pith of the sampled tree as plot center. Since the center of the sampled tree could not be used as a plot center for basal area measurements, a basal area plot was taken three feet from the sampled tree's pith. To maintain randomness, a random bearing was established for the basal area measurement around each tree. Basal area for red spruce species was noted as well as basal area of competing species and total basal area.

### 2.2. Sample processing and dendrochronological analysis

Extracted increment cores were stored in large paper straws and labeled according to the plot number and tree sample number. Cores were oven dried in the laboratory. Properly dried increment cores were mounted to wooden core mounts, pressed, and dried. Mounted cores were then sanded using an electric palm sander. All cores were sanded to a minimum grit level of 400. Sample cores that showed growth suppression were sanded to a grit level of 800.

Sanded increment cores were then visually cross dated by using the list method of Yamaguchi (1991) to track the instances of marker rings. Tree cores were marked by highlighting false, missing, and narrow rings (Yamaguchi 1991). Marker years can be observed as years where the ring width is notably narrow or wide relative to the surrounding tree rings. Once cores were visually cross dated, they were then scanned at an optical resolution of 2400 dots per inch.

Scanned images of the cores were then processed in the tree-ring image analysis program CooRecorder (version 9.0) (CooRecorder and DendroScan: Cybis Elektronik and Data AB, Sweden). CooRecorder was used to measure all tree-ring widths for each increment core. Missing rings were noted in CooRecorder and tree rings were assigned an accurate age. Tree cores were then statistically cross dated using the computer program COFECHA (version 6.06) (Holmes 1983; Grissino-Mayer 2001). COFECHA compares individual tree chronologies to the plot master chronologies and identifies potential errors (i.e., missing rings or false rings) associated with the initial visual crossdating process. Individual chronologies with low correlations to the master chronology could have crossdating errors such as missing rings or improper age of the outermost

**Table 2.** Chronology statistics for the 18 plots.

| Landscape cluster | Site | Interval | Total trees (radii) | Mean ring width (mm) | Absent rings (%) | Mean sensitivity | EPS | EPS ≥0.80 year (trees) |
|---|---|---|---|---|---|---|---|---|
| NLNA | 147 | 1936–2018 | 10 (20) | 1.938 | 0.00 | 0.1449 | 0.87 | 1936 (6) |
| | 16 | 1945–2018 | 10 (20) | 2.440 | 0.00 | 0.1467 | 0.84 | 1945 (5) |
| | 8 | 1947–2017 | 11 (19) | 2.240 | 0.00 | 0.2108 | 0.90 | 1929 (5) |
| NLSA | 115 | 1935–2018 | 10 (20) | 2.188 | 0.00 | 0.1510 | 0.83 | 1949 (7) |
| | 130 | 1941–2018 | 10 (20) | 2.105 | 0.06 | 0.1243 | 0.84 | 1941 (8) |
| | 101 | 1944–2018 | 10 (20) | 2.183 | 0.00 | 0.1299 | 0.83 | 1944 (8) |
| CLNA | 30 | 1968–2017 | 10 (19) | 1.930 | 0.00 | 0.1371 | 0.80 | 1968 (10) |
| | 85 | 1923–2018 | 11 (22) | 1.908 | 0.00 | 0.2159 | 0.82 | 1923 (10) |
| | 128 | 1926–2018 | 10 (20) | 1.271 | 0.07 | 0.1801 | 0.86 | 1900 (7) |
| CLSA | 103 | 1926–2018 | 20 (40) | 1.725 | 0.19 | 0.1247 | 0.86 | 1926 (14) |
| | 61 | 1930–2018 | 10 (19) | 1.228 | 0.11 | 0.1424 | 0.80 | 1930 (10) |
| | 13 | 1939–2018 | 10 (20) | 2.672 | 0.06 | 0.1426 | 0.85 | 1939 (7) |
| SLNA | 106 | 1919–2018 | 10 (19) | 1.719 | 0.05 | 0.1690 | 0.87 | 1919 (7) |
| | 40 | 1921–2018 | 11 (22) | 1.743 | 0.05 | 0.1582 | 0.80 | 1921 (11) |
| | 121 | 1936–2018 | 10 (20) | 1.656 | 0.05 | 0.1697 | 0.84 | 1936 (8) |
| SLSA | 113 | 1914–2018 | 10 (20) | 1.664 | 0.20 | 0.1698 | 0.86 | 1922 (7) |
| | 23 | 1953–2018 | 10 (19) | 2.143 | 0.00 | 0.1167 | 0.85 | 1953 (8) |
| | 142 | 1930–2017 | 10 (20) | 1.498 | 0.20 | 0.2015 | 0.83 | 1930 (9) |

**Note:** Plot level statistics are grouped within their corresponding landscape cluster. Abbreviations for landscape cluster are defined in Table 1. EPS, expressed population symbol. EPS ≥ 0.80 provides the earliest year when the individual chronology reaches an EPS of 0.80 or higher, and also provides corresponding tree count to satisfy EPS ≥ 0.80.

ring (Grissino-Mayer 2001). Once chronologies were statistically cross dated, plot master chronologies were then standardized in computer program ARSTAN version 6.05 P (Cook 1985). ARSTAN is used to standardize chronologies to isolate climate related growth responses while removing and or minimizing growth responses related to competition and other non-climatic factors (Chhin 2015). Cubic smoothing splines are generally used for shade tolerant species in closed canopy stands and trees that have experienced periods of suppression (Cook and Peters 1981). Cubic smoothing splines of 50 years were used for chronologies with average lengths of approximately 100 years. For several plots which consisted of younger cohorts of sampled trees, a cubic smoothing spline of a shorter length of 40 or 30 years was used. Residual chronologies were selected to represent plot level master chronologies in ARSTAN. Residual chronologies consist of plot level growth chronologies that have autocorrelation removed which removes growth trends caused by persistent non-climatic factors. Expressed Population Signal (EPS) is one of the many statistics ARSTAN provides in its output; EPS provides a measure of how well the sample chronology portrays a hypothetically perfect chronology (Magruder et al. 2013). We used an EPS threshold of 0.80, which is considered a benchmark that should be reached for dendroclimatic analysis of red spruce (Kosiba et al. 2017). The primary purpose of calculating EPS in this study was to determine the timeframe for each site chronology that had adequate tree sample replication. We did not use EPS to implicitly infer climatic sensitivity (Buras 2017). A total of 17 of the 18 climate plots reached minimum EPS values of 0.80. Plot 103 did not initially reach an EPS value of 0.80. An additional 10 trees were cored at plot 103 and resulted in an EPS of over 0.85 for the final plot 103 chronology. Landscape cluster chronologies were developed for all six landscape clusters (Fig. 2). Landscape cluster chronologies consisted of averaging each of the individual plots' residual chronologies. Averaged landscape cluster chronologies only included averages for time periods where individual chronologies maintained EPS signals above 0.80. We feel this process ensures that each site has equal weight in the landscape cluster chronology average. We did not pool individual tree-ring series for each tree core in a landscape cluster due to the concern that that trees from some sites may dominate the final chronology of each landscape cluster.

### 2.3. Dendroclimatic analysis

Historic climate data for this project was obtained from Oregon State University's PRISM website (prism.oregonstate.edu) (Daly et al. 2008). Climate data was obtained for each of the 18 study sites by using each plot's geographical coordinates (i.e., latitude and longitude) in PRISM's climate modeling system. Historical climate data obtained from PRISM is spatially interpolated from actual weather stations that have been collecting climate data since 1895 (Daly et al. 2008). Based on a digital elevation model, PRISM is able to capture the physiographic conditions of a study site location by making climate adjustments mainly due to elevation and other topographical positions such as aspect. PRISM in particular has been shown to perform well in estimating climatic conditions in mountainous areas. In our study, we only used the climate data that corresponded with the timeframe in which all landscape clusters had achieved an EPS value greater than 0.80, which was the time period of 1941–2017. Monthly climatic data included total precipitation, mean temperature, minimum temperature, and maximum temperature. Climate moisture index (CMI) is a function of precipitation and temperature which takes into account water losses through evapotranspiration (Hogg 1997). CMI was calculated with monthly data obtained from PRISM. Regional climate values for the six landscape clusters (NLNA, NLSA, CLNA, CLSA, SLNA, and SLSA) were derived from averaging climate values from the three individual plots within each regional group.

Growth–climate analysis was conducted to find significant relationships between residual chronologies for each regional group and the corresponding reginal climate variables including minimum temperatures, maximum temperatures, mean temperatures, precipitation, and climate moisture index. Growth–climate analyses were conducted using a step-wise multiple regression conducted with R (Version 3.6.0) statistical analysis software for the period 1941–2017 (Venables and Ripley 2002; Chhin et al. 2008; R Core Team 2019). Growth–climate analysis consisted of comparing red spruce growth to monthly and seasonal (3 consecutive months) climate variables and creating multiple linear regression models using stepwise analysis (with forward selection) and only including significant predictors with low AIC (Akaike information criterion) values. If significant monthly and seasonal climate values overlapped, the stronger predictor of the two variables was retained in the model and the predictor with the lower prediction power was

**Fig. 2.** Chronologies for each landscape cluster comprising three latitudinal groups (i.e., (*a*) northern, (*b*) central, and (*c*) southern) in combination with two aspects (i.e., north and south). Chronologies in solid gray lines are from landscape clusters with north-facing aspects; chronologies in dashed black lines are from landscape clusters with south-facing aspects.

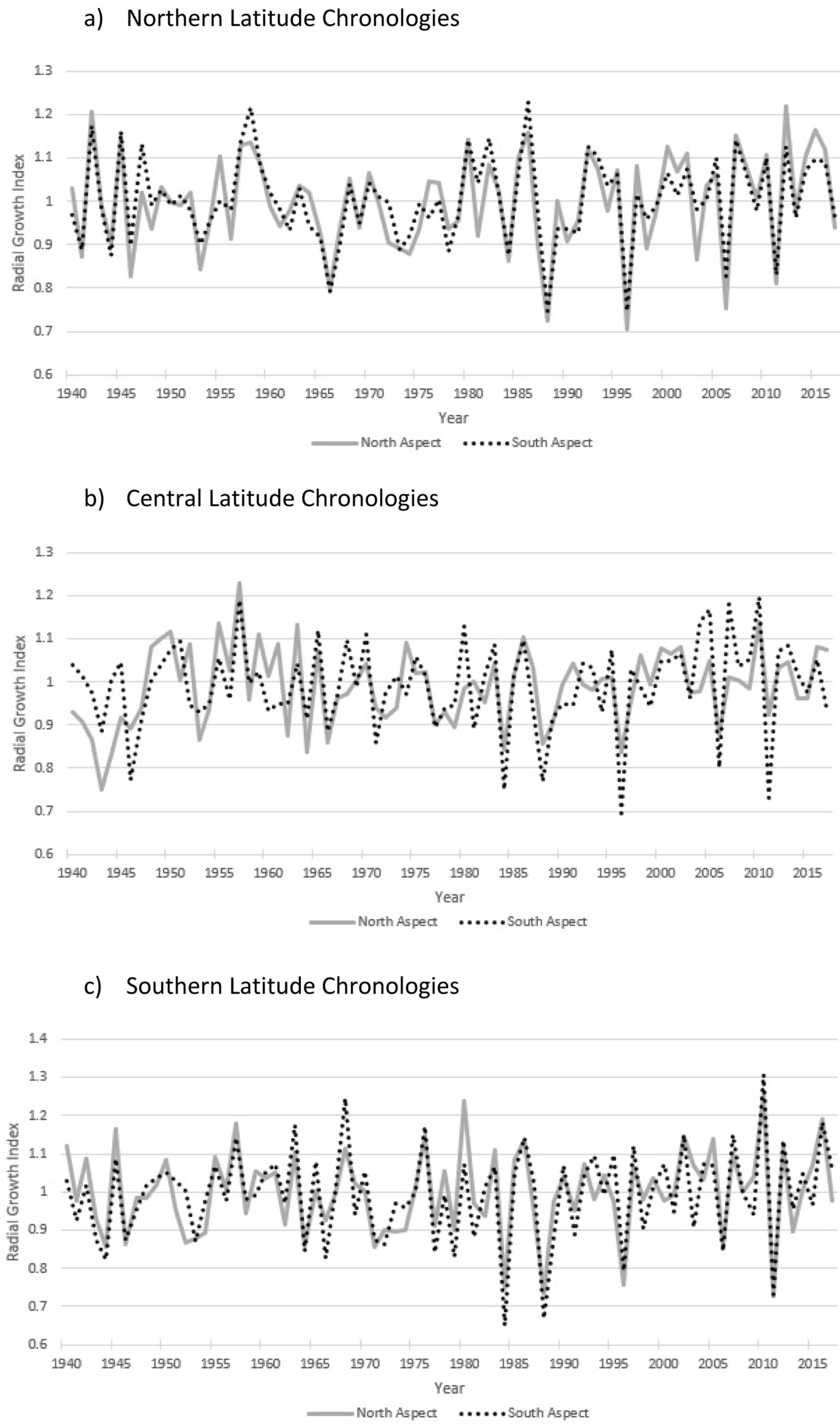

dropped from the regression models. Seasonal variables were considered for regression models as sometimes seasonal variables can show relationships that monthly variables may not. Historic growth–climate analysis also considered climate conditions for the previous growing season as climate conditions during the previous growing season can have impacts on current growth. This lag effect of tree growth was important to consider when determining climate conditions critical to red spruce growth. Growth–climate analysis was conducted over a 76-year time span (i.e., 1941–2017). This time frame was determined when a second member of a regional group lost acceptable EPS signals and an average residual chronology could no longer be constructed. Standardized partial regression coefficients were also calculated to rank the relative importance of the predictor variables in each regression model (Zar 1999).

### 2.4. Future growth projections

Future climate data for the 18 sites were obtained using the computer program ClimateNA (Wang et al. 2006). ClimateNA provides spatially interpolated future climate data that is custom tailored to different emissions scenarios. The climate scenario referred to as Representative Concentration Pathways (RCP) 4.5 was used to make future climate predictions. The climate scenario RCP 4.5 is thought of as a middle of the road scenario in terms of future projected greenhouse trajectories (Wang et al. 2016). Individual climate estimations at each site were averaged for each regional group and were applied to regional chronologies to predict future growth. Table 3 shows average, future predicted climate values for each of the landscape clusters in the central Appalachians.

The historic growth–climate regression equations were then used to project spruce growth on a regional level. Monthly and seasonal projected climate values were included in the regression models to make estimations of future tree growth with the selected climate variables. Climate variables used to project future growth included: mean monthly temperature, minimum temperature, maximum temperature, precipitation, and climate moisture index.

Growth projections were conducted on a yearly basis and then averaged over four, 20-year, periods: 2021–2040, 2041–2060, 2061–2080, and 2081–2100. Projected growth for each time period was then compared with average growth during a 20-year reference period of 1981–2000. The reference period of 2081–2000 was selected because it was a common timeframe shared by all cores and the time period also occurred before many climate change concerns were highlighted. Projected future percent change in growth (relative to the reference period) was determined for each of the time periods for each regional group and also for all landscape clusters combined. Projected change in growth for all groups combined may be used to estimate future growth change for central Appalachian red spruce. Growth projections for landscape clusters could be used to determine areas that may produce favorable red spruce growth in a changing climate. Future projections were compared with a 95% confidence interval of growth during the reference period for each regional group. All changes in growth for the future time periods which surpass positive and negative growth changes within the 95% confidence interval are considered a significant departure in future growth.

## 3. Results

### 3.1. Growth–climate relationships

In terms of latitude, there were was a higher percentage of absent rings in southern landscape clusters, followed by the central and northern landscape clusters (Table 2). Furthermore, within each latitudinal group, more missing rings were present in the south versus north aspect (Table 2). The correlation matrix for all site level chronologies are provided in Supplementary A[1]. All six landscape clusters show negative growth relationships related to mean summer temperatures in the previous growing season ($t-1$) (Fig. 3; Table 4). All six landscape clusters share August ($t-1$) (either as the sole monthly or part of the seasonal climate variable) as negatively related to growth. Landscape clusters NLNA, CLSA, and SLSA, all share the late summer seasonal window ($t-1$) (July, August, and September) as negatively associated with growth. Groups SLNA and CLNA share the summer seasonal window ($t-1$) (June, July, and August) which are also negatively associated with growth. Mean temperatures during the fall and early winter seasonal period ($t-1$) (October, November, and December) are positively associated with growth across all six landscape clusters. A regression model ($R^2$ = 0.225) that uses mean temperature values was developed for all six landscape clusters which had two statistically significant growth predictors. The most important predictor of growth was mean late fall seasonal temperatures ($t-1$) (October, November, and December) which had a positive growth association. The second most important predictor in the model for all regions combined was seasonal summer mean temperatures ($t-1$) (July, August, and September) which had negative growth associations (Fig. 3; Supplementary B[1]).

Comparing regional growth to maximum temperatures yielded regression models with the largest adjusted $R^2$ values compared with all of the climate variables (Fig. 3; Table 4). Maximum seasonal

**Table 3.** Average annual climatic values for the reference period and future growth periods for each landscape cluster and all landscape clusters combined.

| Time period | NLNA | NLSA | CLNA | CLSA | SLNA | SLSA | All |
|---|---|---|---|---|---|---|---|
| **Mean temperature (°C)** | | | | | | | |
| 1981–2000 | 7.74 | 8.00 | 6.60 | 6.93 | 7.83 | 8.24 | 7.55 |
| 2021–2040 | 9.47 | 9.34 | 8.51 | 8.82 | 9.38 | 9.81 | 9.22 |
| 2041–2060 | 10.10 | 10.10 | 9.16 | 10.08 | 10.04 | 10.47 | 10.48 |
| 2061–2080 | 10.73 | 10.64 | 9.22 | 9.48 | 10.64 | 11.07 | 9.88 |
| 2081–2100 | 11.69 | 10.66 | 9.79 | 10.12 | 10.67 | 11.10 | 10.51 |
| **Maximum temperature (°C)** | | | | | | | |
| 1981–2000 | 13.39 | 13.59 | 12.03 | 12.79 | 13.47 | 14.12 | 13.23 |
| 2021–2040 | 15.59 | 16.93 | 14.12 | 14.89 | 15.04 | 15.31 | 15.08 |
| 2041–2060 | 16.28 | 16.89 | 14.74 | 15.53 | 15.64 | 15.90 | 15.72 |
| 2061–2080 | 16.98 | 16.23 | 15.44 | 16.22 | 16.37 | 16.64 | 16.42 |
| 2081–2100 | 16.98 | 15.54 | 15.46 | 16.24 | 16.35 | 16.61 | 16.43 |
| **Minimum temperature (°C)** | | | | | | | |
| 1981–2000 | 2.10 | 2.41 | 1.17 | 1.07 | 2.17 | 2.36 | 1.88 |
| 2021–2040 | 3.35 | 3.22 | 3.00 | 2.85 | 3.82 | 4.42 | 3.44 |
| 2041–2060 | 3.93 | 3.80 | 3.56 | 3.43 | 4.44 | 5.04 | 4.03 |
| 2061–2080 | 4.52 | 4.38 | 4.06 | 3.93 | 4.90 | 5.51 | 4.55 |
| 2081–2100 | 4.52 | 4.39 | 4.13 | 3.99 | 4.99 | 5.60 | 4.60 |
| **Precipitation (mm)** | | | | | | | |
| 1981–2000 | 115.98 | 123.22 | 125.98 | 122.24 | 133.18 | 131.59 | 125.37 |
| 2021–2040 | 124.95 | 125.77 | 126.55 | 122.19 | 125.16 | 125.53 | 125.02 |
| 2041–2060 | 127.82 | 128.69 | 126.85 | 123.38 | 124.43 | 124.67 | 125.97 |
| 2061–2080 | 129.53 | 130.58 | 129.33 | 125.22 | 126.73 | 126.91 | 128.05 |
| 2081–2100 | 137.79 | 138.94 | 138.58 | 134.10 | 135.24 | 135.09 | 136.62 |
| **Climate moisture index (cm)** | | | | | | | |
| 1981–2000 | 6.33 | 6.93 | 8.06 | 7.34 | 8.05 | 7.50 | 7.37 |
| 2021–2040 | 6.01 | 6.17 | 7.11 | 6.24 | 6.52 | 6.49 | 6.44 |
| 2041–2060 | 5.92 | 6.03 | 6.76 | 6.00 | 6.07 | 6.03 | 6.14 |
| 2061–2080 | 5.76 | 5.88 | 6.66 | 5.80 | 5.93 | 5.87 | 5.99 |
| 2081–2100 | 6.54 | 6.67 | 7.57 | 6.70 | 6.79 | 6.71 | 6.83 |

**Note:** Future climate values are estimated from Representative Concentration Pathway (RCP) 4.5 scenario data. Abbreviations for landscape cluster are defined in Table 1.

[1]Supplementary data are available with the article at https://doi.org/10.1139/cjfr-2020-0491.

**Fig. 3.** Significant predictors of the regression models are shown for landscape clusters using temperature climatic variables. Predictors displayed in black indicate a negative association with red spruce growth, while indicators in light gray indicate a positive relationship with red spruce. Adjusted $R^2$ values are listed for each growth model. In models with more than one regression term, the predictor variables are ranked in order of significance, where 1 is assigned to the most influential predictor variable.

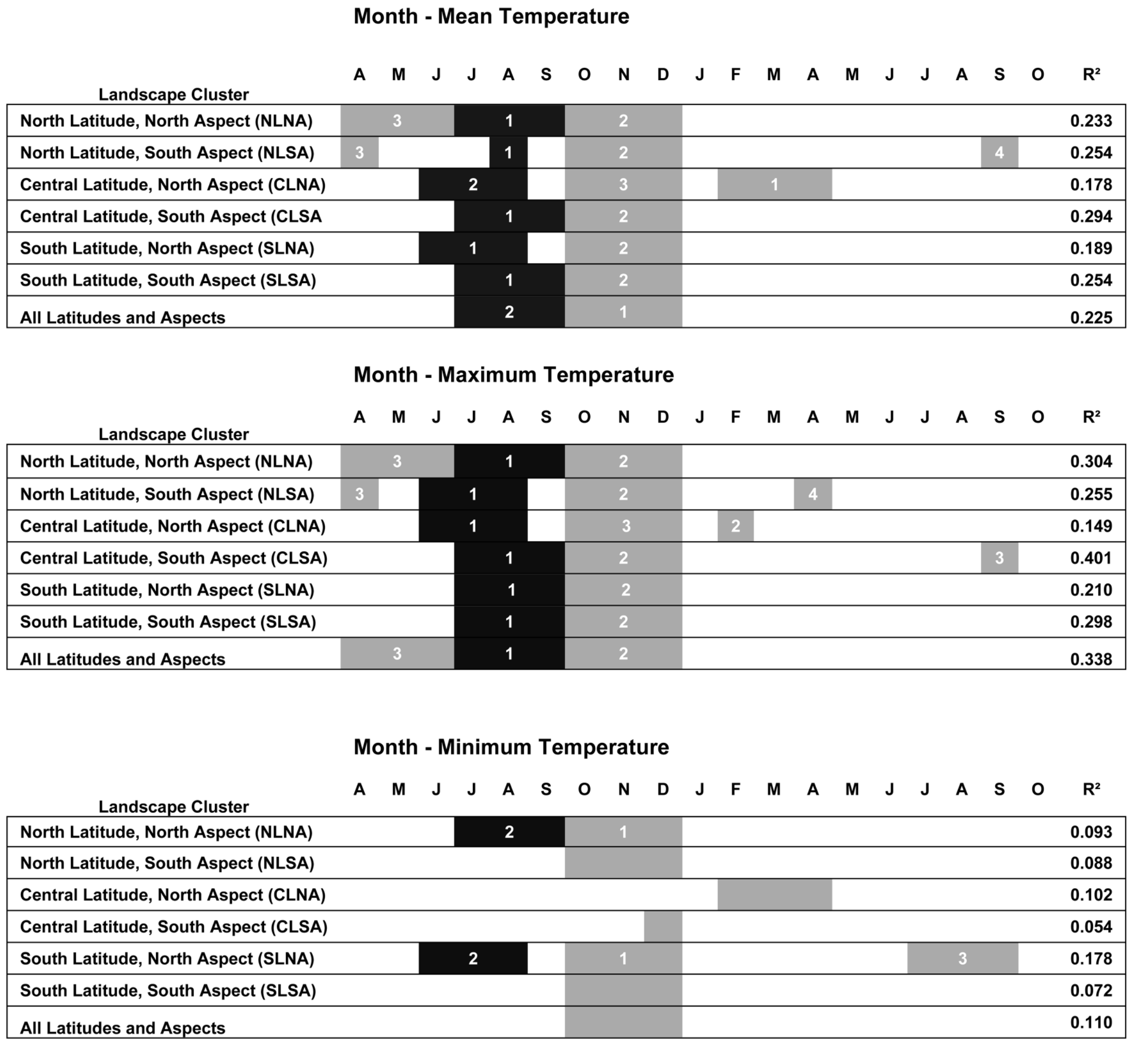


summer temperatures (encompassing different seasonal combinations of June, July, August, and September) for the previous growing season ($t-1$) were important predictors for growth declines in the following growing season. All six landscape clusters shared at least July and August maximum temperatures as part of their 3-month seasonal predictor. NLSA and CLNA both shared June as the third month associated with spruce growth declines in the following year. Landscape clusters NLNA, CLSA, SLNA, and SLSA, all shared September ($t-1$) as the third month for their significant 3-month seasonal window. Landscape clusters NLNA, NLSA, CLSA, and SLSA, all shared the 3-month seasonal window of fall to early winter (October, November, and December) of the previous year ($t-1$) as a positive associated growth predictor. Regional group CLNA included maximum February temperature ($t$) as a positive related growth predictor. The regression model to predict spruce growth using maximum temperatures ($R^2 = 0.338$) for all landscape clusters combined had seasonal summer (July, August, and September) ($t-1$) maximum temperatures as the most important predictor in the model (Fig. 3; Supplementary B[1]). Fall and early winter seasonal (October, November, and December) ($t-1$) maximum temperatures were the second most important predictors in the regression model. The third most important and last predictor in the regression model includes spring seasonal (April, May, and June) ($t-1$) maximum temperatures.

Growth is positively associated with minimum monthly seasonal fall and early winter temperatures (October, November, and December) ($t-1$) (Fig. 3; Table 4). Landscape clusters NLNA, NLSA, SLNA, and SLSA, all shared this period as a significant predictor in their regional regression models. Site CLSA had just minimum temperatures for the month of December ($t-1$) as a significant predictor for spruce growth. The regression model developed to predict growth using minimum temperatures ($R^2 = 0.110$) for all six landscape clusters combined had one significant positively related predictor which is minimum temperatures for the fall and early winter seasonal period ($t-1$) (October, November, and December) (Fig. 3; Supplementary B[1]).

Precipitation had fewer significant predictors associated with radial growth compared with the other moisture variable — Climate Moisture Index (Fig. 4; Table 5). Landscape clusters CLNA and CLSA both experienced a seasonal negative growth relationship with precipitation during the months of July, August, and September ($t$). Plots SLNA and SLSA experienced a monthly negative relationship with precipitation during the month of August ($t$). Landscape clusters located within the northern latitude portion of

**Table 4.** Coefficients for regression models that use temperature climatic variables in predicting red spruce growth for landscape clusters.

| Landscape cluster | C | V1 | B1 | V2 | B2 | V3 | B3 | V4 | B4 |
|---|---|---|---|---|---|---|---|---|---|
| **Mean temperature** | | | | | | | | | |
| NLNA | 1.5892 | −0.0621 | −0.427 | 0.0257 | 0.299 | 0.0298 | 0.221 | — | — |
| NLSA | 0.9900 | −0.0264 | −0.283 | 0.0218 | 0.281 | 0.0150 | 0.225 | 0.0194 | 0.227 |
| CLNA | 1.5433 | 0.0221 | 0.349 | −0.0375 | −0.318 | 0.0171 | 0.269 | — | — |
| CLSA | 1.9754 | −0.0653 | −0.500 | 0.0274 | 0.369 | — | — | — | — |
| SLNA | 1.8869 | −0.0561 | −0.341 | 0.0284 | 0.330 | — | — | — | — |
| SLSA | 1.9105 | −0.0688 | −0.422 | 0.0335 | 0.341 | 0.0179 | 0.213 | — | — |
| All latitudes and aspects | 1.6272 | 0.0270 | 0.387 | −0.0434 | −0.366 | — | — | — | — |
| **Maximum temperature** | | | | | | | | | |
| NLNA | 1.5570 | −0.0615 | −0.546 | 0.0227 | 0.301 | 0.0351 | 0.315 | — | — |
| NLSA | 1.5161 | −0.0431 | −0.398 | 0.0201 | 0.302 | 0.0131 | 0.258 | 0.0102 | 0.203 |
| CLNA | 1.5456 | 0.0112 | 0.352 | −0.0272 | −0.302 | 0.0080 | 0.266 | — | — |
| CLSA | 1.8506 | −0.0588 | −0.578 | 0.0207 | 0.304 | 0.0129 | 0.188 | — | — |
| SLNA | 1.8628 | −0.0473 | −0.440 | 0.0234 | 0.315 | — | — | — | — |
| SLSA | 2.2192 | −0.0638 | 0.508 | 0.0279 | 0.330 | — | — | — | — |
| All latitudes and aspects | 1.6523 | −0.0536 | −0.583 | 0.0210 | 0.341 | 0.0207 | 0.228 | — | — |
| **Minimum temperature** | | | | | | | | | |
| NLNA | 1.3611 | 0.0262 | 0.313 | −0.0294 | −0.234 | — | — | — | — |
| NLSA | 1.0358 | 0.0247 | 0.317 | — | — | — | — | — | — |
| CLNA | 1.0920 | 0.0221 | 0.338 | — | — | — | — | — | — |
| CLSA | 1.0624 | 0.0096 | 0.258 | — | — | — | — | — | — |
| SLNA | 1.1434 | 0.0262 | 0.323 | −0.0362 | −0.277 | 0.0301 | 0.299 | — | — |
| SLSA | 1.0431 | 0.0263 | 0.296 | — | — | — | — | — | — |
| All latitude and aspects | 1.0362 | 0.0238 | 0.349 | — | — | — | — | — | — |

**Note:** Abbreviations for landscape cluster are defined in Table 1. Coefficients of model predictors are listed in order of importance in the model. C is the model constant. V are model predictors for each climate variable. B is the beta coefficient for each model predictor. c.f. Figure 3 for specific monthly and (or) seasonal variables. Predictor V1 is the most important predictor for each model.

**Table 5.** Coefficients for regression models that use moisture-related climatic variables in predicting red spruce growth for landscape clusters.

| Landscape cluster | C | V1 | B1 | V2 | B2 |
|---|---|---|---|---|---|
| **Precipitation** | | | | | |
| NLNA | 0.9940 | 0.0004 | 0.304 | −0.0004 | −0.275 |
| NLSA | 0.8171 | 0.0003 | 0.323 | 0.0005 | 0.243 |
| CLNA | 0.9841 | −0.0003 | −0.284 | 0.0003 | 0.270 |
| CLSA | 1.1311 | −0.0004 | −0.308 | — | — |
| SLNA | 1.0731 | −0.0005 | −0.243 | — | — |
| SLSA | 1.0884 | −0.0007 | −0.272 | — | — |
| All latitudes and aspects | 0.9671 | 0.0003 | 0.321 | −0.0003 | −0.265 |
| **Climate moisture index** | | | | | |
| NLNA | 1.0198 | 0.0036 | 0.334 | −0.0034 | −0.266 |
| NLSA | 0.9720 | 0.0028 | 0.319 | — | — |
| CLNA | 0.9168 | −0.0023 | −0.265 | 0.0032 | 0.259 |
| CLSA | 0.9878 | 0.0027 | 0.268 | −0.0030 | −0.249 |
| SLNA | 1.0273 | −0.0028 | −0.231 | — | — |
| SLSA | 0.9618 | 0.0028 | 0.264 | — | — |
| All latitudes and aspects | 0.9827 | 0.0032 | 0.358 | −0.0029 | −0.264 |

**Note:** Abbreviations for landscape cluster are defined in Table 1. Coefficients of model predictors are listed in order of importance in the model. C is the model constant. V are model predictors for each climate variable. B is the beta coefficient for each model predictor. c.f. Figure 4 for specific monthly and (or) seasonal variables. Predictor V1 is the most important predictor for each model.

the MNF experience significant growth increases with high precipitation during June, July, and August ($t-1$). The regression model to explain red spruce growth across all landscape clusters combined using precipitation ($R^2$ = 0.143) has two predictors: (*i*) seasonal summer period ($t-1$) (June, July, August), which is positively associated with growth and the most important predictor, and (*ii*) seasonal fall precipitation ($t$) (August, September, October), which is negatively associated with spruce growth (Fig. 4; Supplementary C[1]).

Climate moisture index values for the summer ($t-1$) showed positive relationships with red spruce growth for four of the six landscape clusters (NLNA, NLSA, CLSA, and SLSA) (Fig. 4; Table 5). NLNA, NLSA, and SLSA, share the summer seasonal ($t-1$) months of June, July, and August, while CLSA shares the months of July and August with the previously listed groups. High climate moisture index values in the late summer to early fall ($t$) is negatively associated with growth on three of the six landscape clusters (CLNA, CLSA, SLNA). CLSA and SLNA include the seasonal early fall months ($t$) (August, September, and October) as significant growth predictors. Regional group CLNA includes the seasonal late summer months ($t$) (July, August, and September) as significant predictors in its regression model. The regression model created to predict spruce growth across all landscape clusters combined with CMI values ($R^2$ = 0.178) has the seasonal summer period ($t-1$) (May, June, July) as the most important predictor. The second most important, negatively associated, growth predictor was the seasonal fall and early winter period ($t$) (October, November, December) (Fig. 4; Supplementary C[1]).

### 3.2. Future climate and growth projections

Future predicted growth when considering expected mean monthly temperatures shows significant changes in growth for all landscape clusters except regional group CLNA (Fig. 5). NLNA shows a significant decline in growth for the time period 2061–2080. NLSA is the only regional group NLSA shows positive growth departures during the time periods of 2061–2080 and 2080–2100. Largest growth declines are predicted for regional group CLSA, where significant negative changes in growth are expected for all four future time periods (from 2020–2100). Regional group SLNA is projected to have negative changes in growth with significant declines occurring in time periods 2041–2060, 2061–2080,

**Fig. 4.** Significant predictors of the regression models are shown for landscape clusters using moisture climatic variables. Predictors displayed in black indicate a negative association with red spruce growth, while indicators in light gray indicate a positive relationship with red spruce. Adjusted $R^2$ values are listed for each growth model. In models with more than one regression term, the predictor variables are ranked in order of significance, where 1 is assigned to the most influential predictor variable.

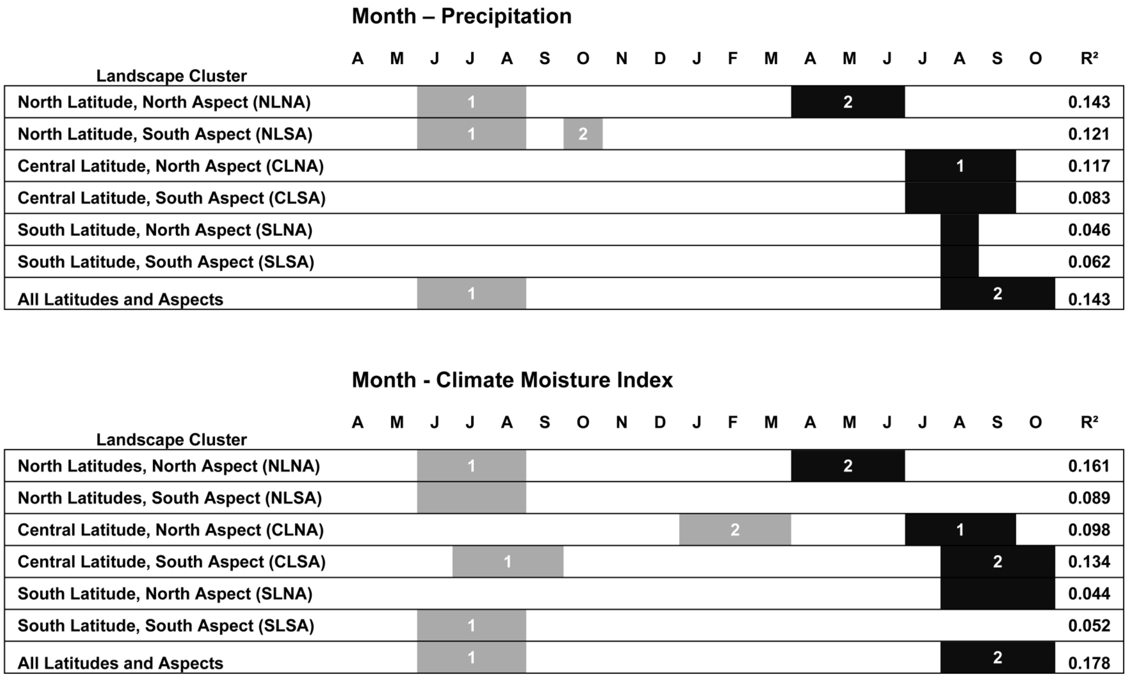




and 2081–2100. SLSA future growth also follows negative trends and significant growth declines are predicted for all four time periods. The overall change in growth for all landscape clusters shows significant growth declines for time periods 2041–2060, 2061–2080, and 2081–2100. Trends in projected growth show the largest declines in growth during the time period 2061–2080, with less negative growth during the last growing period (2081–2100).

Predicting growth using projected maximum monthly temperatures show similar trends as mean temperature but with overall larger declines (Fig. 5). Group NLNA experienced a negative change in growth for all future time periods with significant growth declines in time periods 2041–2060, 2061–2080, and 2081–2100. NLSA shows a significant decline in growth only for the time period of 2081–2100. Regional group CLNA shows significant negative changes in projected growth for all four time periods (2021–2040, 2041–2060, 2061–2080, and 2081–2100). The largest declines in growth are expected to occur at plots in the CLSA group. The CLSA group had significant growth declines for all four time periods with a maximum change in growth during period 2061–2080 where growth is expected to decline by over −14%. Groups NLSA and CLNA overall have smaller predicted growth declines when compared with the other landscape clusters. Predicted growth using maximum monthly temperature for all landscape clusters combined will result in an overall growth decline with significant growth declines in the latter three time periods (2041–2060, 2061–2080, and 2081–2100).

A positive growth trend is observed when projecting future growth with minimum monthly temperatures as the climate predictor (Fig. 5). The southernmost groups (SLNA and SLSA) show the largest positive change in predicted growth with growth changes being significant for all four time periods. Groups NLSA and CLSA have significant positive changes in growth during the last time period (2081–2100). CLNA also has a positive change in future growth when projected using minimum temperature for the last three time periods (2041–2060, 2061–2080, and 2081–2100). Regional group NLNA shows no significant changes in projected growth using minimum temperatures as a predictor. Future projected growth for all landscape clusters combined using future predicted minimum monthly temperatures shows significant overall growth increases in all four time periods (2021–2040, 2041–2060, 2061–2080, and 2081–2100).

For all six landscape clusters and for all landscape clusters combined, projected growth using either future precipitation or climate moisture index did not significantly depart from the baseline growth rates for the reference period of 1980–2000 (Fig. 6).

## 4. Discussion

### 4.1. Growth–climate relationships

It was interesting to note in this study that missing rings were generally more common in more southerly landscape clusters on south aspects. These results suggest that red spruce in the central Appalachians appears to be more physiologically stressed in these typically drier and hotter landscape clusters. Given the high shade tolerance of red spruce, missing rings are generally competition induced (Seymour and Fajvan 2001; Yetter et al. 2021). While missing rings are mentioned in other studies of red spruce, the exact number or percentage is generally not reported (e.g., Goelz et al. 1999), or absent rings are never mentioned as a cross-dating issue (e.g., Kosiba et al. 2017).

The results indicated that historical monthly maximum temperatures were the most important predictors of spruce growth, as these models had the highest $R^2$ values overall for historic growth–climate analyses. A lagged, negative relationship with summer maximum and mean temperatures in the previous year ($t$ − 1) (July, August, and September) suggests that higher temperature could lead to respiratory depletion of carbohydrate reserves necessary for next year's growth (Pallardy 2007; McGuire et al. 2010). High maximum and mean summer temperatures could potentially

**Fig. 5.** Projected red spruce growth by landscape cluster using temperature variables. Error bars indicate a 95% confidence interval of the base growth rate for the reference period of 1980–2000. All changes in growth that lie outside of the error bars indicate significant departures in future growth. Growth projections were created with future climate data that was estimated using climate change scenario data from Representative Concentration Pathway (RCP) 4.5.

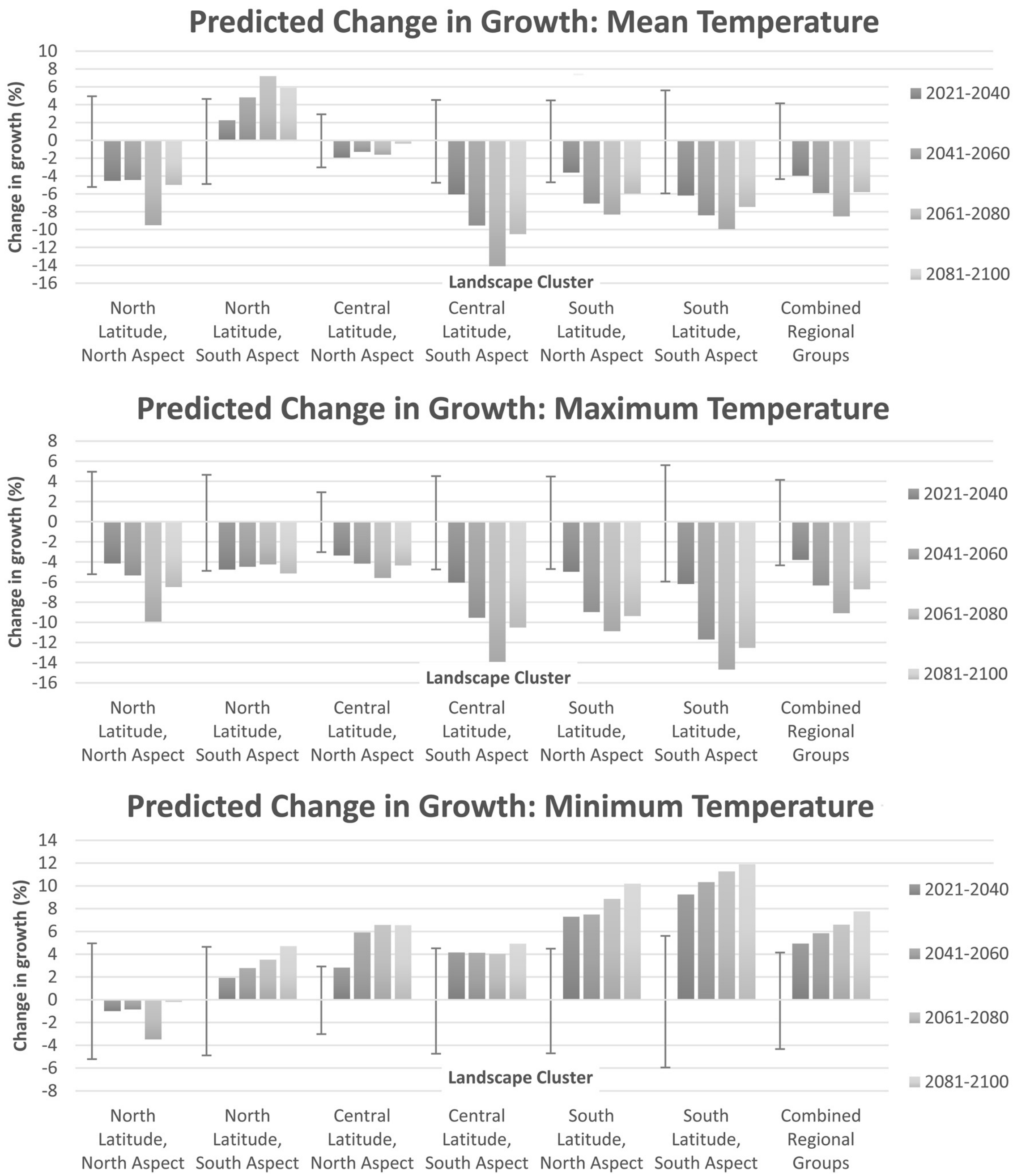


also induce moisture stress from increased evapotranspiration demands (McGuire et al. 2010; Berry and Smith 2014; Schwab et al. 2018). These moisture deficiencies can result in negative growth the following year (Dumais and Prévost 2007). The effect of moisture stress was also underscored by a positive growth response of red spruce in all regions combined to summer ($t-1$) (June, July, and August) precipitation and moisture index. Other studies have shown that radial growth of red spruce populations had negative dendroclimatic relationships with high summer temperatures (Koo et al. 2014; Ribbons 2014). In contrast, Kosiba et al. (2018) found that increasing mean summer temperatures resulted in a positive growth response; this difference in response compared with our study may be due to the fact that the study by Kosiba et al. (2018) was conducted on red spruce trees in the northern portion of its range. Mathias and Thomas (2018) also found that increasing summer temperatures had positive effects on central Appalachian red spruce growth, but only when combined with additional $CO_2$ enrichment. Higher $CO_2$ availability could lead to increased water-use efficiency (Wang et al. 2006), which could, in turn, offset the intensity of temperature induced drought stress. The results suggested a potential aspect effect only for responses to minimum temperature; namely, only northern aspect plots in the northern and southern latitudinal

**Fig. 6.** Projected red spruce growth by landscape cluster using moisture variables. Error bars indicate a 95% confidence interval of the base growth rate for the reference period of 1980–2000. All changes in growth that lie outside of the error bars indicate significant departures in future growth. Growth projections were created with future climate data that was estimated using climate change scenario data from Representative Concentration Pathway (RCP) 4.5.

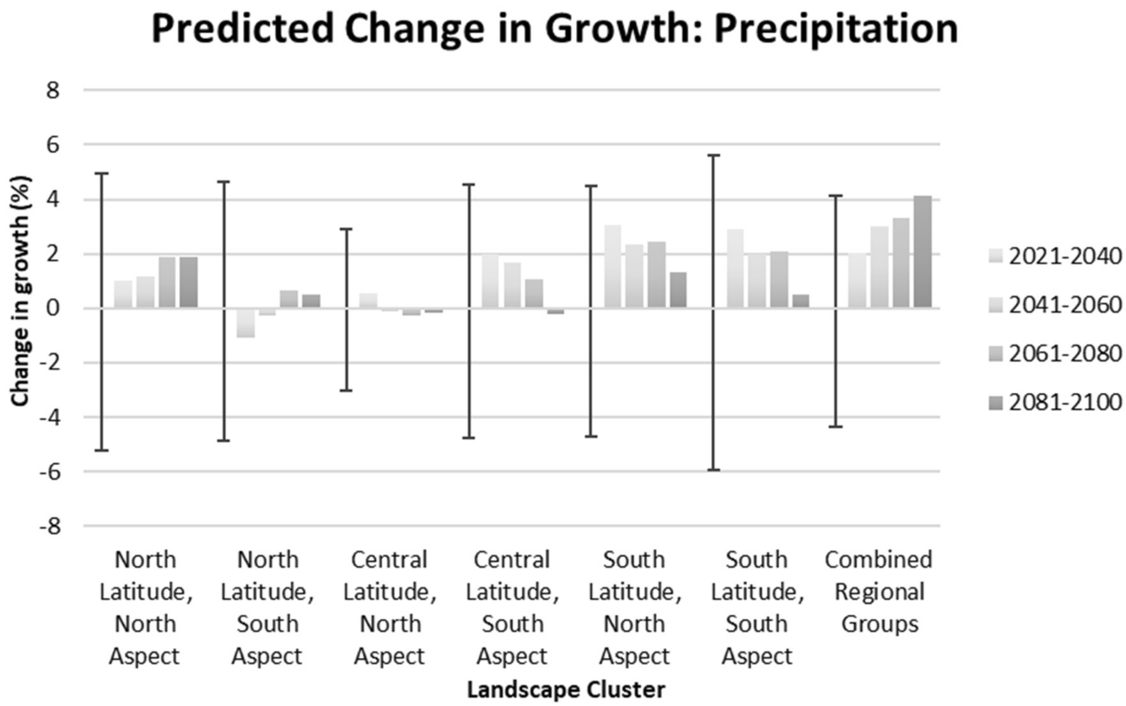


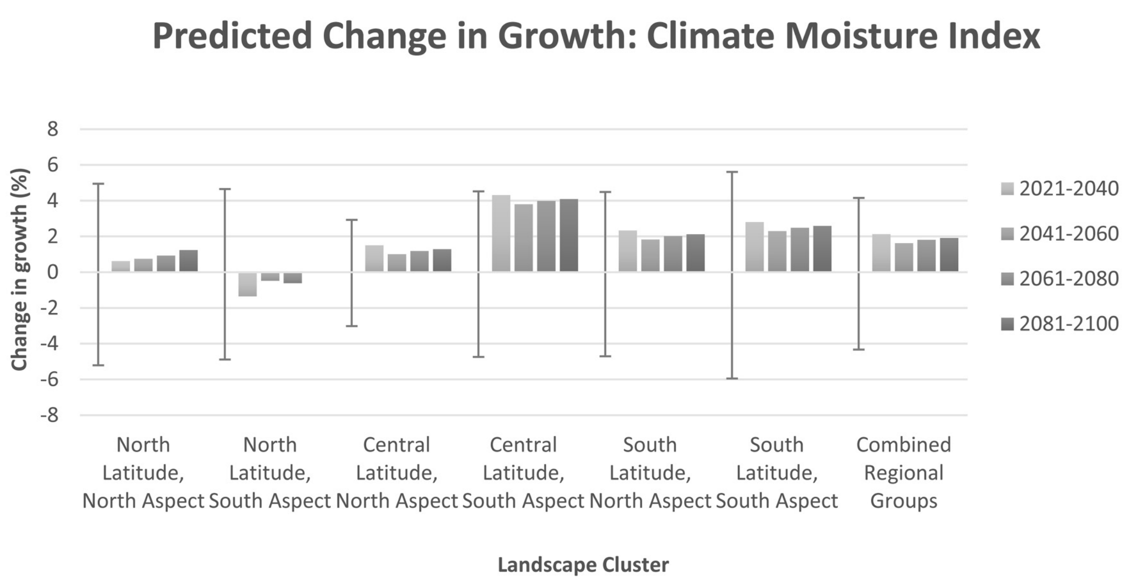


regions experienced negative growth relationships with increasing summer minimum temperatures ($t-1$). This is partly expected, since red spruce experiencing northern aspect microclimates are generally expected to be more acclimated to cooler conditions (Fekedulegn et al. 2003).

Radial growth–climate relationships of red spruce in the central Appalachian region also suggest the potential impact of the length of the growing season. This was reflected in the positive association between radial growth of all regions combined to fall and early winter minimum, mean and maximum temperature conditions in the prior year ($t-1$) (October, November, and December) as well as with maximum temperature in spring and early summer ($t-1$) (April, May, and June). Increases in minimum, mean, and maximum temperatures during these seasonal periods further increase the number of suitable days within the growing season to photosynthesize (Kosiba et al. 2018). Furthermore, the extended growing season of the prior year potentially allows trees to store more carbohydrates and establish better buds for next year's growth (Kozlowski et al. 1991). Increasing minimum, mean, and maximum temperatures, especially in the early winter growing season, also result in milder winters. Milder winters will result in less xylem cavitation, which allows better productivity by not impairing stem hydraulic conductivity (Holst et al. 2008). Other studies have confirmed that red spruce responded favorably to an extended growing season into the fall (Gunderson et al. 2012; Kosiba et al. 2018). In particular, Mathias and Thomas (2018) found that warming temperatures at the beginning or end of the growing season extremes result in increased growth in central Appalachian red spruce. Furthermore, Butnor et al. (2019) found that warmer spring temperatures allowed red spruce bud break to occur earlier in the growing season and resulted in a positive growth response. The results suggested a latitudinal effect since only red spruce from the northern latitudinal regions of the study (NLNA and NLSA) showed a positive relationship with mean and maximum spring and early summer temperatures and reinforces the importance of warm conditions at the beginning of the growing season to foster growth for more northern populations of red spruce.

The negative association between fall precipitation and the climatic moisture index and radial growth current growing season (*t*) is unusual but could be due to crown damage from heavy fall snowfall or high wind events associated with precipitation events (Peterson 2000; Griscom et al. 2014). White et al. (2014) also found that precipitation events could have negative impacts on red spruce growth but only in the spring. Another explanation for the inverse relationship between radial growth and precipitation and moisture index is that excessive moisture, especially within the soil, could potentially lead to unfavorable anoxic conditions, as five of the 18 plots have soils which are poorly drained (White et al. 2014). North latitude, south aspect red spruce did not respond negatively to increased precipitation and moisture; it is speculated that plots in this regional group are not affected by excess precipitation because their soils are well drained or because the south-facing aspect facilitates evaporation (Parker 1982).

### 4.2. Growth projections

Future growth projections provide some insight on how spruce will perform with future climate predictions. Our future growth projections using either precipitation or climate moisture index indicate that there will be no significant change in future growth. In contrast, growth projections using future mean and maximum temperatures suggest that future climate conditions will not favor red spruce growth. These results support predictions that red spruce habitat will decrease with future climate change (Rentch et al. 2007; Walter et al. 2017). Growth declines related to mean and maximum temperature in the future could be caused by increased respiration in summer months (Ribbons 2014). Koo et al. (2014) found that increasing temperatures will also lead to growth declines in southern Appalachian spruce, and these predictions align with our growth projections. However, our results using future minimum temperatures show conflicting changes. Growth increases are predicted due to increasing minimum temperatures. These future increases will be the result of an extended growing season which will allow spruce to put on more radial growth, provided that maximum temperatures do not have a larger negative effect on growth (Gunderson et al. 2012; Kosiba et al. 2018; Mathias and Thomas 2018).

NLSA and CLNA landscape clusters show the least overall growth declines when considering future maximum and mean temperatures. These two landscape clusters showed either growth increases or no change with minimum temperature, precipitation, and climate moisture index. These results may indicate that locations either in central latitudes on north aspects or northern latitudes on south aspects will be the best for red spruce growth in the future. An important fact to note is that the large significant declines in growth associated with mean and maximum temperature or precipitation do not occur until the third time period of 2061–2080. If greenhouse emissions are further reduced, less severe growth declines could be observed.

## 5. Conclusion

Radial growth of central Appalachian red spruce was negatively associated with increased mean and maximum summer temperatures. High temperatures in the fall showed positive effects on red spruce growth across all regions, likely due to an extended growing season. Fall precipitation events have negative growth impacts on red spruce. Growth declines from increasing summer temperatures may be mitigated by the positive growth impacts resulting from an expanded growing season in the future. Radial growth projections indicate that red spruce in the northern latitude portion on south-facing aspects as well as central latitudes on north aspects of the central Appalachians are expected to be resilient to future climate change. Restoration efforts in the future may benefit from considering future growth projections for central Appalachian red spruce when planning future restoration activities.

## Acknowledgements

We thank Kevin Nixon and John Holden for assistance with field data collection and sample processing. We appreciate the feedback from Dr. Jamie Schuler on a prior version of the manuscript. Two anonymous reviewers also provided constructive feedback on prior version of the manuscript. This project was primarily funded through a Joint Venture Agreement with the United States Department of Agriculture (USDA) Forest Service, Northern Research (Project No. 17-JV-11242301-086). This work was also supported by the USDA, National Institute of Food and Agriculture (NIFA), McIntire Stennis Project No. 1017946, to Sophan Chhin.

## References

Berry, Z.C., and Smith, W.K. 2012. Cloud pattern and water relations in *Picea rubens* and *Abies fraseri,* southern Appalachian Mountains, USA. Agric. For. Meteorol. **162–163**: 27–34. doi:10.1016/j.agrformet.2012.04.005.

Berry, Z.C., and Smith, W.K. 2014. Experimental cloud immersion and foliar water uptake in saplings of *Abies fraseri* and *Picea rubens*. Trees-Struct. Funct. **28**(1): 115–123. doi:10.1007/s00468-013-0934-5.

Blum, B.M. 1990. *Picea rubens* Sarg. Red spruce. In Silvics of North America. *Edited by* R.M. Burns and B.H. Honkala (tech cords). Vol. 1. Conifers. Agriculture Handbook 654. U.S. Department of Agriculture. Washington, DC, USA.

Buras, A. 2017. A comment on the expressed population signal. Dendrochronologia, **44**: 130–132. doi:10.1016/j.dendro.2017.03.005.

Butnor, J.R., Verrico, J.R., Johnsen, B.M., Maier, K.H., Christopher, A., and Vankus, V. 2019. Phenotypic variation in climate-associated traits of red spruce (*Picea rubens sarg.*) along elevation gradients in the southern Appalachian Mountains. Castanea, **84**(2): 128–143. doi:10.2179/0008-7475.84.2.128.

Byers, E.A., Love, K.C., Haider, K.R., Burks, E.J., and Rowan, J.E., 2013. Red spruce (*Picea rubens*) cover in West Virginia. Version 1.0. West Virginia Division of Natural Resources GIS Clearing House. Available from http://wvgis.wvu.edu/data/dataset.php.

Chhin, S. 2015. Impact of future climate change on a genetic plantation of hybrid pine. Botany, **93**: 397–404. doi:10.1139/cjb-2015-0014.

Chhin, S., Hogg, E.H., Lieffers, V.J., and Huang, S. 2008. Influences of climate on the radial growth of lodgepole pine in Alberta. Botany, **86**: 167–178. doi:10.1139/B07-120.

Cook, E.R. 1985. A time series analysis approach to tree ring standardization. Ph.D. thesis, University of Arizona.

Cook, E.R., and Peters, K. 1981. The smoothing spline: a new approach to standardizing forest interior tree-ring width series for dendroclimatic studies. Tree-Ring Bull. **41**: 45–53.

Daly, C., Halbleib, M., Smith, J.I., Gibson, W.P., Doggett, M.K., Taylor, G.H., et al. 2008. Physiologically sensitive mapping of climatological temperature and precipitation across the conterminous United States. Int. J. Climatol. **28**: 2031–2064. doi:10.1002/joc.1688.

Dumais, D., and Prévost, M. 2007. Management for red spruce conservation in Quebec: The importance of some physiological and ecological characteristics – A review. For. Chronical, **83**(3): 378–392. doi:10.5558/tfc83378-3.

Fekedulegn, D., Hicks, R.R., and Colbert, J.J. 2003. Influence of topographic aspect, precipitation and drought on radial growth of four major tree species in an Appalachian watershed. For. Ecol. Manage. **177**(3): 409–425. doi:10.1016/S0378-1127(02)00446-2.

Fritz, H.R. 1976. Tree rings and climate. The Blackburn Press, Tuscon, AZ, USA.

Gavin, D.G., Beckage, B., and Osborne, B. 2008. Forest dynamics and the growth decline of red spruce and sugar maple on Bolton Mountain, Vermont: a comparison of modeling methods. Can. J. For. Res. **38**: 2635–2649. doi:10.1139/X08-106.

Goelz, J.C.G., Burk, T.E., and Zedaker, S.M. 1999. Long-term growth trends of red spruce and faser fir at Mt. Rogers, Virginia and Mt. Mitchell, North Carolina. For. Ecol. Manage. **115**: 49–59. doi:10.1016/S0378-1127(98)00435-6.

Griscom, H.P., Griscom, B.G., and Siderhurst, L. 2014. Spatial dynamics and the growth decline of red spruce and sugar maple on Bolton Mountain, Vermont: A comparison of modeling methods. Can. J. For. Res. **34**(1): 99–104. doi:10.1139/X08-106.

Grissino-Mayer, H.D. 2001. Evaluating crossdating accuracy: a manual and tutorial for the computer program COFECHA. Tree-Ring Res. **57**(2): 205–221.

Gunderson, C.A., Edwards, N.T., Walker, A.V., O'Hara, K.H., Campion, C.M., and Hanson, P.J. 2012. Forest phenology and a warmer climate – Growing season extension in relation to climate provenance. Glob. Change Biol. **18**(6): 2008–2025. doi:10.1111/j.1365-2486.2011.02632.x.

Hogg, E.H. 1997. Temporal scaling of moisture and the forest-grassland boundary in western Canada. Agric. For. Meteorol. **84**: 115–122. doi:10.1016/S0168-1923(96)02380-5.

Holmes, R.L. 1983. Computer-assisted quality control in tree-ring dating and measurement. Tree-Ring Bulletin, **43**: 69–75.

Holst, J., Barnard, R., Brandes, E., Buchmann, N., Gessler, A., and Jaeger, L. 2008. Impacts of summer water limitation on the carbon balance of a Scots pine forest in the southern upper Rhine plain. Agricultural and Forest Meteorology, **148**: 1815–1826. doi:10.1016/j.agrformet.2008.06.008.

Johnson, D.M., and Smith, W.K. 2006. Low clouds and cloud immersion enhance photosynthesis in understory species of a southern Appalachian spruce-fir forest (USA). Am. J. Bot. **93**(11): 1625–1632. doi:10.3732/ajb.93.11.1625. PMID:21642107.

Koo, K.A., Patten, B.C., Teskey, R.O., and Creed, I.F. 2014. Climate change effects on red spruce decline mitigated by reduction in air pollution within its shrinking habitat range. Ecol. Modell. **293**: 81–90. doi:10.1016/j.ecolmodel.2014.07.017.

Kosiba, A.M., Schaberg, P.G., Rayback, S.A., and Hawley, G.J. 2017. Comparative growth trends of five northern hardwood and montane tree species reveal divergent trajectories and response to climate. Can. J. For. Res. **47**: 743–754. doi:10.1139/cjfr-2016-0308.

Kosiba, A.M., Schaberg, P.G., Rayback, A.R., and Hawley, G.K. 2018. The surprising recovery of red spruce growth shows links to decreased acid deposition and elevated temperature. Sci. Total Environ. **637–638**(2018): 1480–1491. doi:10.1016/j.scitotenv.2018.05.010. PMID:29801241.

Kozlowski, T.T., Kramer, P.J., and Pallardy, S.G. 1991. The physiological ecology of woody plants. Academic Press, San Diego, CA, USA.

Magruder, M., Chhin, S., Palik, B., and Bradford, J.B. 2013. Thinning increases climatic resilience of red pine. Can. J. For. Res. **43**(9): 878–889. doi:10.1139/cjfr-2013-0088.

Mathias, J.M., and Thomas, R.B. 2018. Disentangling the effects of acidic air pollution, atmospheric $CO_2$, and climate change on recent growth of red spruce trees in the Central Appalachian Mountains. Glob. Change Biol. **24**(24): 3938–3953. doi:10.1111/gcb.14273.

McGuire, A.D., Ruess, R.W., Lloyd, A., Yarie, J., Clein, J.S., and Juday, G.P. 2010. Vulnerability of white spruce tree growth in interior Alaska in response to climate variability: dendrochronological, demographic, and experimental perspectives. Can. J. For. Res. **40**: 1197–1209. doi:10.1139/X09-206.

Nauman, T.W., Thompson, J.A., Teets, S.J., Dilliplane, T.A., Bell, J.W., Connolly, S.J., et al. 2015. Ghosts of the forest: mapping pedomemory to guide forest restoration. Geoderma, **247–248**: 51–64. doi:10.1016/j.geoderma.2015.02.002.

Pallardy, S.G. 2007. Physiology of woody plants. 3rd ed. Academic Press, San Diego, CA, USA.

Parker, A.J. 1982. The topographic relative moisture index: an approach to soil-moisture assessment in mountain terrain. Phys. Geogr. **3**(2): 160–168. doi:10.1080/02723646.1982.10642224.

Pauley, T.K. 2008. The Appalachian Inferno: historical causes for the disjunct distribution of *Plethedon nettingi* (Cheat Mountain Salamander. Northeast. Nat. **15**(4): 595–606. doi:10.1656/1092-6194-15.4.595.

Peterson, C.J. 2000. Catastrophic wind damage to North American forests and the potential impact of climate change. Sci. Total Environ. **262**(1): 287–311. doi:10.1016/S0048-9697(00)00529-5. PMID:11087033.

R Core Team. 2019. R: A language and environment for statistical computing. R Foundation for Statistical Computing, Vienna, Austria. Available from http://www.R-project.org/.

Rentch, J.S., Schuler, T.M., Ford, W.M., and Nowacki, G.J. 2007. Red spruce stand dynamics, simulations, and restoration opportunities in the Central Appalachians. Restor. Ecol. **15**(3): 440–452. doi:10.1111/j.1526-100X.2007.00240.x.

Rentch, J.S., Ford, F.M., Schuler, T.S., Palmer, J., and Diggins, C.A. 2016. Release of suppressed red spruce using canopy gap creation – Ecological restoration in the Central Appalachians. Nat. Areas J. **36**(1): 29–37. doi:10.3375/043.036.0108.

Ribbons, R.R. 2014. Disturbance and climatic effects on red spruce community dynamics at its southern continuous range margin. PeerJ, **2**(e293). doi:10.7717/peerj.293. PMID:24688869.

Schwab, N., Kaczka, R., Janecka, K., Böhner, J., Chaudhary, R., Scholten, T., and Schickhoff, U. 2018. Climate change-induced shift of tree growth sensitivity at a central Himalayan treeline ecotone. Forests, **9**: 267. doi:10.3390/f9050267.

Seymour, R.S., and Fajvan, M.A. 2001. Influence of prior growth suppression and soil on red spruce site index. North. J. Appl. For. **18**: 55–62. doi:10.1093/njaf/18.2.55.

Speer, J.H. 2012. Fundamentals of tree-ring research. University of Arizona Press, Tuscon, AZ, USA.

Stephenson, S.L. 2013. A natural history of the Central Appalachians. West Virginia University Press, Morgantown, WV, USA.

Theobald, D.M., Stevens, D.L., Jr., White, D., Urquhart, N.S., Olsen, A.R., and Norman, J.R. 2007. Using GIS to generate spatially balanced random survey designs for natural resources applications. Assess. Manage. **40**: 134–146. doi:10.1007/s00267-005-0199-x.

Thomas-Van Gundy, M., Strager, M., and Rentch, J. 2012. Site characteristics of red spruce witness tree locations in the uplands of West Virginia, USA. J. Torrey Bot. Soc. **139**(4): 391–405. doi:10.3159/TORREY-D-11-00083.1.

Thomas-Van Gundy, M.A., and Sturtevant, B.R. 2014. Using scenario modeling for red spruce restoration planning in West Virginia. J. For. **112**(5): 457–466. doi:10.5849/jof.13-087.

Trapp, S.E., Smith, W.P., and Flaherty, E.A. 2017. Diet and food availability of the Virginia northern flying squirrel (*Glaucomys sabrinus fuscus*): implications for dispersal in a fragmented forest. J. Mammal. **98**(6): 1688–1996. doi:10.1093/jmammal/gyx115.

Venables, W.N., and Ripley, B.D. 2002. Modern applied statistics with S. 4th ed. Springer, New York, USA.

Walter, J.A., Neblett, J.C., Atkins, J.W., and Epstein, H.E. 2017. Regional and watershed scale analysis of red spruce habitat in the southeastern United States: implications for future restoration efforts. Plant Ecol. **218**: 305–315. doi:10.1007/s11258-016-0687-5.

Wang, G.G., Chhin, S., and Bauerle, W.L. 2006. The effect of natural atmospheric $CO_2$ fertilization suggested by open-grown white spruce in a dry environment. Glob. Change Biol. **12**: 601–601. doi:10.1111/j.1365-2486.2006.01098.x.

Wang, T., Hamann, A., Spittlehouse, D., and Carroll, C. 2016. Locally downscaled and spatially customizable climate data for historical and future periods for North America. PLoS One, **11**(6): e0156720. doi:10.1371/journal.pone.0156720. PMID:27275583.

White, P.B., Soule, P., and van de Gevel, S. 2014. Impacts of human disturbance on the temporal stability of climate–growth relationships in a red spruce forest, southern Appalachian Mountains, USA. Dendrochronology, **32**: 71–77. doi:10.1016/j.dendro.2013.10.001.

Yamaguchi, D. 1991. A simple method for cross-dating increment cores from living trees. Can. J. For. Res. **21**: 414–416. doi:10.1139/x91-053.

Yetter, E., Brown, J., and Chhin, S. 2021. Anamorphic site index curves for Central Appalachian red spruce in West Virginia, USA. Forests, **12**: 94. doi:10.3390/f12010094.

Zar, J.H. 1999. Biostatistical analysis. 4th ed. Prentice Hall, Upper Saddle River, NJ, USA.